

# ChemBioChem

## Supporting Information

### **Surface Display of Complex Enzymes by *in Situ* SpyCatcher-SpyTag Interaction**

Sabrina Gallus, Theo Peschke, Malte Paulsen, Teresa Burgahn, Christof M. Niemeyer, and Kersten S. Rabe\*© 2020 The Authors. Published by Wiley-VCH Verlag GmbH & Co. KGaA. This is an open access article under the terms of the Creative Commons Attribution Non-Commercial NoDerivs License, which permits use and distribution in any medium, provided the original work is properly cited, the use is non-commercial and no modifications or adaptations are made.

## Contents

### Materials and Methods

Contains details about plasmid construction, amino acid sequences, bacterial growth conditions, surface display of fluorescent proteins, proteinase K treatment, expression analysis and investigation of SC-ST interaction, whole-cell biocatalytic activity assays, as well as immunofluorescence microscopy and flow cytometry analysis conducted during this study. Includes the following tables:

Table S1:	Plasmids used in this study
Table S2:	Sequences of primers used in this study
Table S3:	Amino acid sequences of functional proteins used in this study

### Supplementary Figures

Figure S1:	Design of genetic constructs
Figure S2:	Proteinase K treatment of cells displaying RFP-ST
Figure S3:	Fluorescence microscopic investigation of intercellular cross-coupling events
Figure S4:	Western blot analysis of the SC-ST interaction
Figure S5:	Scheme for whole-cell biocatalytic activity assays
Figure S6:	Biocatalytic activity assays with permeabilized cells
Figure S7:	Fluorescence microscopy images of <i>E. coli</i> expressing mRFP-ST and Lpp-OmpA-eGFP-SC after 20 h
Figure S8:	BM3 whole-cell biocatalytic activities of a non-coupling control
Figure S9:	Verification of Gre2p and GDH surface exposure by immunofluorescence microscopy
Figure S10:	Flow cytometry analysis of BM3 displaying cells
Figure S11:	Expression analysis and whole-cell biocatalytic activity assay for cells expressing Lpp-OmpA-BM3
Figure S12:	Design of the GDH variant carrying an internal ST

### References

## Materials and Methods

**Plasmid construction.** All plasmids used in this study and their sources are listed in Table S1 and the design of genetic constructs is illustrated in Figure S1 and Figure S12. All plasmid constructions were carried out using the isothermal recombination as described by Gibson et al.<sup>[1]</sup> PCR-products or synthetic DNA-fragments were inserted into linearized vector backbones via 30 base pair homologous sequence overlaps. The sequences of all primers utilized for the PCR amplifications are listed in

Table S2. The assembly reaction was performed at 50 °C for 1 h under continuous shaking. Subsequently, the reaction mixtures were treated with DpnI to remove any remaining vector from prior PCR reactions and transformed into chemical competent *E. coli* DH5 $\alpha$  cells and selected on LB-agar plates containing 100  $\mu$ g/ml ampicillin or 30  $\mu$ g/ml chloramphenicol at 37 °C for at least 12 h. All plasmids were purified using ZR Plasmid Miniprep-Classic (Zymo Research) according to the manufacturer's instructions. Plasmid Sequences were verified by commercial sequencing (LGC genomics). The amino acid sequences of all functional proteins are listed in Table S3.

**pTF16\_lpp-ompA-eGFP-SC.** A pTF16 backbone employing a N-terminal lpp-ompA fusion and a C-terminal SC was amplified using primers SG19 and SG20 with pTF16\_lpp-ompA-SC as the template. This backbone was then recombined with an eGFP encoding insert, which had been generated by PCR using the primers SG21 and SG22 with pET\_SC-eGFP-his<sub>6</sub> as the template.

**pTF16\_lpp-ompA-BM3-his<sub>6</sub>.** A pTF16 backbone employing a N-terminal lpp-ompA fusion was amplified using primers TP17 and TP18 with pTF16\_lpp-ompA-ST as the template. This backbone was then recombined with an insert encoding for P450 BM3(F87A), which had been generated by PCR using the primers TP21 and TP22 with pEXP42\_P450-BM3-F87A as the template. The resulting plasmid was PCR amplified using the primers SG03 and SG04 to introduce a C-terminal his<sub>6</sub>. The mutations A74G and F87V were introduced by site-directed mutagenesis using the primers KSR168 and KSR169.

**pTF16\_lpp-ompA-BM3-myc.** The plasmid pTF16\_lpp-ompA-BM3-his<sub>6</sub> was PCR amplified using the primers SG40 and SG41 in order to replace his<sub>6</sub> with a myc epitope tag.

**pET\_mRFP-ST-his<sub>6</sub>.** A pET backbone employing a C-terminal ST and his<sub>6</sub> was amplified using primers SG09 and SG10 with pET\_Gre2p-ST-his<sub>6</sub> as the template. This backbone was then recombined with an insert encoding for mRFP,<sup>[2]</sup> which was ordered as a codon-optimized gene fragment (GeneArt Gene Synthesis, Thermo Fisher Scientific).

**pET\_GDH(ST-his<sub>6</sub>).** The plasmid pET\_GDH-his<sub>6</sub> was PCR amplified using the primers P26 and P27 in order to remove the amino acids D202 and P203 and insert the ST sequence with the aid of primer overhangs. The resulting plasmid pET\_GDH(ST)-his<sub>6</sub> was then amplified using the primers P28 and P29 to remove the C-terminal his<sub>6</sub>. The internal his<sub>6</sub> sequence was subsequently inserted by PCR amplification using the primers P30 and P31 to obtain pET\_GDH(ST-his<sub>6</sub>).

**pET\_BM3-ST-his<sub>6</sub>.** A pET backbone encoding for a C-terminal ST and his<sub>6</sub> was amplified using primers TP27 and TP28 with pET\_Gre2p-ST-his<sub>6</sub> as the template. This backbone was then recombined with an insert encoding for P450 BM3(F87A), which had been generated by PCR using the primers TP35 and TP36 with pEXP42\_P450-BM3-F87A



SG39	TCGCTGATCAGTTTCTGTTACCTTTGGTCGGTTTATATGCATCCAC
SG40	GAACAGAACTGATCAGCGAAGAAGATCTGTAATGAGATCCGGCTGCTAACAAAGCC
SG41	TCGCTGATCAGTTTCTGTTACCCCCAGCCCACACGTCTTTTGC
TP17	GCTACCACCACCACCACACCATTATC
TP18	TAATGAGATCCGGCTGCTAACAAAGC
TP21	CCGGATAATGGTGTGGGTGGTGGTAGCACAAATTAAGAAATGCCTCAGCCAAAAAC
TP22	TCGGGCTTTGTTAGCAGCCGGATCTCATTACCCAGCCCACACGTCTTTTGC
TP27	CATATGTATATCTCCTTCTTAGTACAACTTGTGATATTCCTTCTTAAAG
TP28	GGTGGTGGTGGTAGCGCCCATATTGTTATGGTGGATGCATATAAAC
TP35	AGTTTGTACTAAGAAGGAGATATACATATGACAATTAAGAAATGCCTCAGCCAAAAAC
TP36	CATAACAATATGGGCGCTACCACCACCACCAGCCCACACGTCTTTTGC

**Table S3: Amino acid sequences of functional proteins used in this study.**

Functional protein	Amino acid sequence
Lpp-OmpA	MKATKLVLGAVILGSTLLAGCSSNAKIDQGINPYVGFEMGYDWLGRMPYKGSVENGAY KAQGVQLTAKLGYFITDDLDIYTRLGGMVWRADTKSNVYGNHDTGVSPVFAAGGVEY AITPEIATRLEYQWTNNIGDAHTIGTRPDNGV
SpyTag	AHIVMVDAYKPTK
SpyCatcher	VDTLSGLSSEQGQSGDMTIEEDSATHIKFSKRDEDGKELAGATMELRDSSGKTISTWIS DGQVKDFYLYPGKYTFVETAAPDGYEVATAITFTVNEQGQVTVNGKATKGDAMI
eGFP	VSKGEELFTGVVPIVELDGDVNGHKFSVSGEGEGDATYGKLTGKLFICTTGKLPVPWPT LVTTLYGVQCFSRYPDHMKQHDFFKSAMPEGYVQERTIFFKDDGNYKTRAEVKFEG DTLVNRIELKGFDFKEDGNILGHKLEYNYNHNVYIMADKQKNGIKVNFKIRHNIEDGSV QLADHYQQNTPIGDGPVLLPDNHVLSLQSSALSQKDPNEKRDMVLLFVTAAGITLGM ELYK
mRFP	MASSEDVIKEFMRFKVRMEGSVNGHEFEIEGEGEGRPYEGTQTAKLKVTGGPLPFA WDILSPQFQYGSKAYVKHPADIPDYLLKLSFPEGFKWERVMNFEDGGVTVTQDSSLQ DGEFIYKVKLRGTNFPDGPVMQKKTMGWEASTERMYPEDGALKGEIKMRLKLDGG HYDAEVKTTYMAKKPVQLPGAYKTDIKLDITSHNEDYTIVEQYERAEGRHSTGA
Gre2p	MSVFSVSGANGFIAQHIVDLLKEDYKVIGSARSQEKAENLTEAFGNPNFNSMEIVPDISK LDAFDHVFQKHGKEIKIVLHTASPFCDITDSDERDLLIPAVNGVKGILHSIKKYAADSVER VVLTSYAAVFDMAKENDKSLTFNEESWNPATWESCQSDPVSAAYCGSKKFAEKAWE FLEENRDAVKFELTAVNPVYVFGPQMFQKDVKKHLNLSCELVNSLMHLSPEDKIPELFG GYIDVRDVAKAHLVAFQKRETIGQRLIVSEARFTMQDVLIDLNDFPILKGNIPVKGPGS GATHNTLGATLDNKKSKLLGFKFRNLKETIDDTASQILKFEGR
GDH	MYPDLKGVVAITGAASGLGKAMAIRFGKEQAKVVINYYSNKQDPNEVKEEVKAGGE AVVVQGDVTKVEDVKNIVQTAIKEFGTLDIMINNAGLENPVPSHEMPLKDWKDVIGTNL TGAFVLSREAIKYFVENDIKGNVINMSSVHEVIPWPLFVHYAASKGGIKLMTETLALEYA PKGIRVNNIGPGAINTPINAIEKFAADPKQKADVESMIPMGYIGEPPEEIAAVWLASKESS YVTGITLFAADGGMTKYPFQAGRG
BM3(A74G F87V)	MTIKEMPQPKTFGELKNLPLLNTDKPVQALMKIADELGEIFKFEAPGRVTRYLSSQRLIK EACDESRFDKNLSQGLKVRDFAGDGLATSWTHEKNWKAHNILLPSFSQQAMKGYH AMMVDIAVQLVQKWERLNADEHIEVPEDMTRLTLDITGLCGFNRYRNSFYRDQPHFIT SMVRLADEAMNKLQRANPDDPAYDENKRQFQEDIKVMNDLVDKIIADRKASGEQSDDL LTHMLNGKDPETGEPLDDENIRYQIITFLIAGHETTSGLLSFALYFLVKNPHVLQKAAEEA ARVLVDPVPSYKQVKQLKYVGMVLNEALRLWPTAPAFSLYAKEDTVLGGEYPLEKGD LMVLIPQLHRDKTIWGDVEEFRPERFENPSAIPQHAFKPFNGQRACIGQQFALHEAT LVLGMLLKHDFDFEDHTNYELDIKETLTKPEGFVVKAKSKKIPLGGIPSPSTEQSACKVR KKAENAHNTPLLVLVYGSNMGTAEGTARDLADIAMSKGFAPQVATLDHAGNLPREGAV LIVTASYNGHPPDNAKQFVDWLDQASADEVKGVRSVFGCGDKNWATTYQKVPFID ETLAAKGAENIADRGEADASDDFEGTYEEWREHMWSDVAAYFNLDIENSEDNKSTLSL QFVDSAADMPLAKMHGAFSTNVVASKELQPPGSARSTRHLEIELPKEASYQEGDHLG VIPRNYEGIVNRVTARFGLDASQIRLEAEELKLAHLPLAKTVSVEELLQYVELQDPVTR TQLRAMAAKTVCPPHKVELEALLEKQAYKEQVLAKRLTMLELLEKYPACEMKFSEFIAL LPSIRPRYYSISSSPRVDEKQASITVSVSGEAWSGYGEYKGIASNYLAELQEGDTITCF ISTPQSEFTLPKDPETPLIMVGPVGTGVAPFRGFVQARKQLKEQQQSLGEAHLVYFGCRS PHEDYLYQEELENAQSEGIITLHTAFSRMPNQPKTYVQHVMEQDGKLIELLDQGAHFY ICGDGSQMAPAVEATLMKSYADVHVQSEADARLWLQQLLEEKGRYAKDVWAG

**Bacterial growth conditions:** *E. coli* BL21(DE3) cells were transformed with the plasmids listed in the respective method sections by using electroporation. The cells were selected overnight on LB/agar plates containing appropriate antibiotics (100 µg/ml ampicillin, 30 µg/ml chloramphenicol) at 37 °C. Liquid cultures of 5 ml LB<sup>+antibiotics</sup> were generated from clones of the LB/agar plates and cultured overnight for 14-18 h at 37 °C, 180 rpm in culture tubes. Two flasks with 20 ml LB<sup>+antibiotics</sup> were inoculated with 0.5 ml overnight culture respectively. The cultures were incubated at 37 °C, 180 rpm until an OD<sub>600</sub> of 0.6 was reached. For experiments investigating the SC-ST display system or the corresponding non-coupling controls one of the cultures was induced with 1 mM IPTG for cytosolic expression of passenger-ST fusions and the second culture was induced with 1 mM IPTG for expression of passenger-ST and 1 mM L-arabinose for expression of Lpp-OmpA-SC or Lpp-OmpA-ST fusions. For experiments investigating the conventional display system one culture was kept uninduced and the second culture was induced with 1 mM L-arabinose for expression of Lpp-OmpA-passenger fusions. Subsequently the cells were incubated at 25 °C until further analysis.

**Surface display of fluorescent proteins.** To investigate the co-localization of Lpp-OmpA-eGFP-SC and mRFP-ST cells were transformed with plasmids pTF16\_lpp-ompA-eGFP-SC and pET\_mRFP-ST-his<sub>6</sub> and cultures were grown and induced as described above. For investigation of intercellular cross-coupling events, cells were transformed with pTF16\_lpp-ompA-SC and pET\_ST-eGFP-his<sub>6</sub> or pTF16\_lpp-ompA-SC and pET\_mRFP-ST-his<sub>6</sub>. Liquid cultures were grown as described above until an OD<sub>600</sub> of 0.6 was reached. Subsequently the cultures were mixed in equal amounts and induced as described above. 6 h or 20 h after induction 600 µl of the cells were harvested and resuspended in 100 µl LB<sup>+antibiotics</sup>. 10 µl of the cell suspensions were analyzed using a Zeiss Axiovert 200M fluorescence microscope equipped with the software Axio Vision 4.7. The eGFP signal was analyzed with a FITC filter set (green channel) and the mRFP signal with a rhodamine filter set (red channel).

**Proteinase K Treatment.** Cells were transformed with plasmids pTF16\_lpp-ompA-eGFP-SC and pET\_mRFP-ST-his<sub>6</sub> and cultures were grown and induced as described above. 6 h after induction cells were harvested, washed with PBS buffer (11.5 mM sodium phosphate, 50 mM NaCl, pH 7.3) and resuspended in PBS buffer to a final OD<sub>600</sub> of 8. Subsequently 1 mg/ml proteinase K was added, incubated for 10 min and inactivated by adding 5 mM phenylmethylsulfonyl fluoride (PMSF). Cells were washed three times with PBS and analyzed by western blot analysis as described in section “Expression analysis and investigation of SC-ST interaction”.

**Expression analysis and investigation of SC-ST interaction.** Cells were transformed with the following plasmids:

Gre2p:	pTF16_lpp-ompA-SC and pET_Gre2p-ST-his <sub>6</sub>	(SC-ST display system)
GDH:	pTF16_lpp-ompA-SC and pET_GDH-ST-his <sub>6</sub>	(SC-ST display system)
BM3:	pTF16_lpp-ompA-SC and pET_BM3-ST-his <sub>6</sub>	(SC-ST display system)
	or pTF16_lpp-ompA-BM3-his <sub>6</sub>	(conventional display system)

Cultures were grown and induced as described above. 20 h after induction cells were harvested, resuspended in PBS and adjusted to a final OD<sub>600</sub> of 8. 4x Laemmli sample buffer was added and samples were sonicated for 15 s and incubated at 95 °C for 10 min. Proteins were separated on SDS-PAGE (15% (w/v) acrylamide for Gre2p and GDH, 12% (w/v) acrylamide for BM3) and visualized by staining with Coomassie Brilliant Blue G-250. For western blot analysis an identical gel was electroblotted onto a PVDF membrane (VWR). The

membrane was incubated with a mouse anti-His<sub>6</sub> antibody (His Tag antibody orb68952, Biorbyt) at a 1:2000 dilution and a secondary anti-mouse antibody conjugated to alkaline phosphatase (Goat Anti-Mouse IgG Alkaline Phosphatase AP-112, Columbia Biosciences) at a 1:5000 dilution. Subsequently, the blot was developed with a colorimetric reagent (AP Conjugate substrate kit, Biorad).

**Whole-cell biocatalytic activity assays.** Cells were transformed with the following plasmids:

Gre2p:	pTF16_lpp-ompA-SC and pET_Gre2p-ST-his <sub>6</sub>	(SC-ST display system)
GDH:	pTF16_lpp-ompA-SC and pET_GDH-ST-his <sub>6</sub>	(SC-ST display system)
BM3:	pTF16_lpp-ompA-SC and pET_BM3-ST-myc	(SC-ST display system)
	or pTF16_lpp-ompA-ST and pET_BM3-ST-myc	(non-coupling control)
	or pTF16_lpp-ompA-BM3-myc	(conventional display system)
GDH with internal tag:	pTF16_lpp-ompA-SC and pET_GDH(ST-his <sub>6</sub> )	(SC-ST display system)

Cultures were grown and induced as described above. 20 h after induction the cells were harvested by centrifugation at 1,000 x g for 10 min at 4 °C, resuspended in KP<sub>i</sub> (100 mM potassium phosphate, pH 7.5) or Tris buffer (100 mM Tris, pH 8.1) and the OD<sub>600</sub> was adjusted to 5.0. KP<sub>i</sub> buffer was used for cells displaying Gre2p or GDH and Tris buffer was used for cells displaying BM3. For experiments with permeabilized cells the suspensions were incubated with 2% toluene for 40 min at 4°C. The suspensions of intact or permeabilized cells were mixed in microtiter plates (F96 Polysorb Nunc Plate, Thermo Fisher Scientific) with substrates as stated below and the enzymatic reactions were started by adding the cofactors NADPH or NADP<sup>+</sup>. Samples were incubated at 30 °C and substrate/cofactor conversion was followed with the aid of fluorescence read-outs in time intervals of 60 s using a monochromator-based multi-mode microplate reader (Synergy H1, BioTek Instruments GmbH). Samples were shaken between measurements to avoid cell sedimentation. Whole-cell activities were obtained from at least two independent experiments. Details on substrates and cofactors, read-out wavelengths and data analysis are given below. Schematic representations of the assay read-outs can be found in Figure S5.

**Gre2p whole-cell biocatalytic activity.** Activities were determined using the substrate 5-nitrononane-2,8-dione (**1**) that was synthesized as described previously.<sup>[7]</sup> Cell suspensions were diluted to an OD of 0.5 in a total volume of 100 µl KP<sub>i</sub> buffer with 10 mM of substrate (**1**) and 1 mM NADPH (Carl Roth). The decrease in NADPH fluorescence was followed using an excitation wavelength of 340 nm and an emission wavelength of 455 nm. Conversion of fluorescence intensities to NADPH concentrations was conducted using calibration samples with concentrations of 1 mM, 0.75 mM, 0.5 mM, 0.25 mM, 0.1 mM, 10 µM, 1 µM and 0 µM NADPH.

**GDH whole-cell biocatalytic activity.** Cell suspensions were diluted to an OD of 0.5 in a total volume of 100 µl KP<sub>i</sub> buffer with 100 mM D-Glucose (**3**) (Carl Roth) and 1 mM NADP<sup>+</sup> (Carl Roth). The increase in NADPH fluorescence was determined using an excitation wavelength of 340 nm and an emission wavelength of 455 nm. The fluorescence intensities were converted to product amounts using calibration samples of the reaction product NADPH in total amounts ranging from 0 to 15 nmol.

**BM3 whole-cell biocatalytic activity.** Activities were determined using a surrogate substrate as described by Neufeld et al.<sup>[8]</sup> The cell suspensions were diluted in microtiter

plates to an OD of 0.25 in a total volume of 200  $\mu$ l Tris buffer with 100  $\mu$ M 12-(4-trifluoromethylcoumarin-7-yloxy)dodecanoic acid (**5**) and 1 mM NADPH. Stock solutions of substrate (**5**) were prepared in dimethyl sulfoxide (DMSO) and accounted for 1% of the final assay samples. Formation of the fluorescent product 7-hydroxy-4-trifluoromethylcoumarin (**7**) was followed using an excitation wavelength of 420 nm and an emission wavelength of 500 nm. Fluorescence intensities were converted to product amounts using calibration samples of the fluorescent product (**7**) (Sigma-Aldrich) in total amounts ranging from 0 to 400 pmol.

**Immunofluorescence microscopy.** Suspensions of cells ( $OD_{600}$  of 5.0 in  $KP_i$  or Tris buffer) that were induced for surface expression of passengers were prepared as described in section "Whole-cell biocatalytic activity assays". 100  $\mu$ l of the suspensions were incubated with a fluorescently labeled antibody against Myc (Myc Tag Monoclonal Antibody (Myc.A7) DyLight488 MA1-21316-D488, Invitrogen) or His<sub>6</sub> (6x-His Tag Monoclonal Antibody (4E3D10H2/E3) Alexa Fluor488 MA1-135-A488, Invitrogen) at a 1:100 dilution for 1 h at room temperature under continuous shaking. Using three cycles of pelleting and washing the cells in 0.5 ml  $KP_i$  or Tris buffer, the cells were finally resuspended in 100  $\mu$ l of the corresponding buffer. 10  $\mu$ l of the cell suspension was analyzed by fluorescence microscopy using a FITC filter set (green channel).

**FACS analysis.** Cells were stained by fluorescently labeled anti-Myc antibodies as described in the section "Immunofluorescence microscopy". Flow cytometry analysis was conducted with a MoFloXDP (Beckman Coulter) using a custom laser setup; 488nm at 400mW Sabr-Coherent. Data were analyzed using the software FlowJo V10 (BD Biosciences). In order to determine the viability, definite numbers of cells were sorted in single-cell mode on a 70 $\mu$ m/60psi setup onto LB/agar plates containing 30  $\mu$ g/ml chloramphenicol and grown overnight at 37 °C. Subsequently the grown colonies were counted using the "Colony Counter" Plugin of the software ImageJ.



## Supplementary Figures

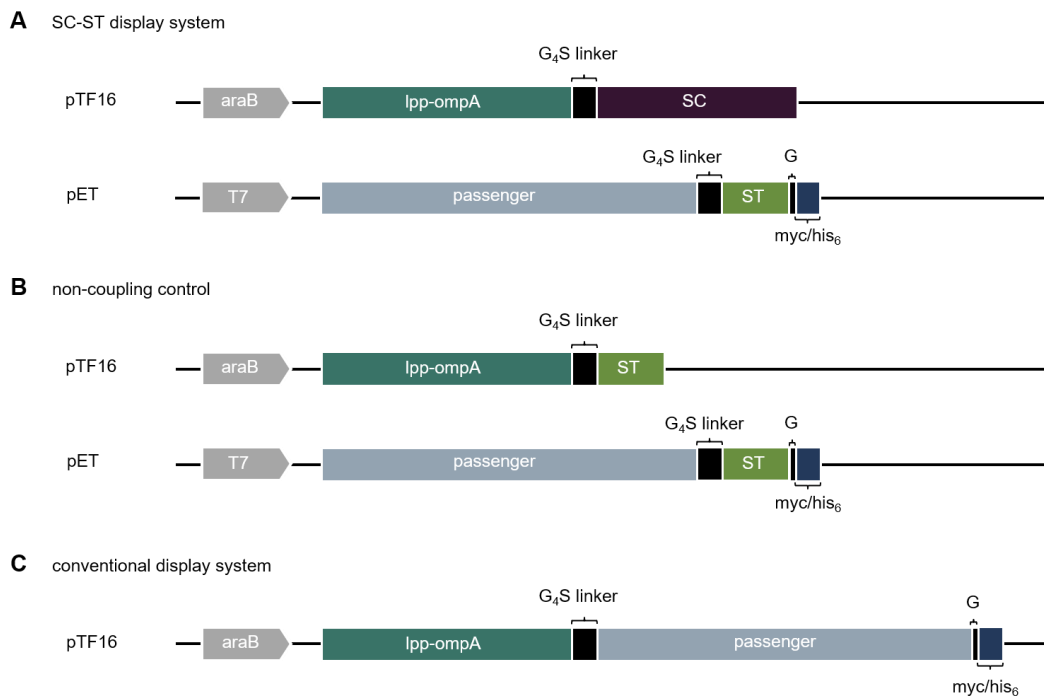


**Figure S1.** Design of genetic constructs for the presentation of passengers on *E. coli* employing the SC-ST display system (**A**), the corresponding non-coupling control (**B**) and the conventional display system (**C**). All fusion genes were designed with a (glycine)<sub>4</sub>-serine sequence (G<sub>4</sub>S) as a flexible linker between the gene-encoding sequences. For the passenger enzyme GDH a double (G<sub>4</sub>S) linker was used.<sup>[5]</sup> To enable analyses by immunostaining, Myc or His<sub>6</sub> affinity tags were added to all fusions containing a passenger. The tags were separated from gene sequences by a single glycine (G). All Lpp-OmpA fusions were encoded on pTF16 derived plasmids, enabling tight control of the expression using the L-arabinose inducible araB promoter. Passenger-ST fusions were encoded on a compatible pET derived plasmid employing an IPTG inducible T7 promoter.

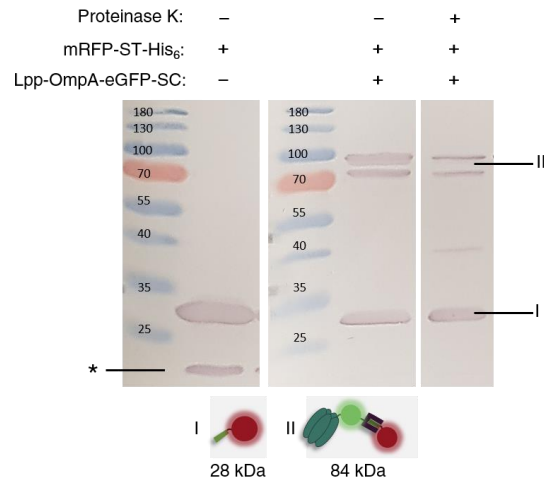


**Figure S2.** Proteinase K treatment of cells displaying mRFP-ST. Whole-cells were incubated with proteinase K, which is not able to penetrate into intact cells. Subsequently cell lysates were separated by SDS-PAGE (15% (w/v) acrylamide) and transferred to a PVDF membrane. The passenger mRFP-ST was detected using primary mouse anti-His<sub>6</sub> antibodies and secondary anti-mouse antibodies conjugated to alkaline phosphatase. Successful conjugation of the passenger mRFP-ST (I) to the membrane anchor via SC-ST interaction is indicated by formation of higher molecular weight bands (II) detected after expression of Lpp-OmpA-eGFP-SC. The occurrence of a double band is presumably due to conjugation of Lpp-OmpA-eGFP-SC to a mRFP-ST degradation product (\*), which is also present in samples without expression of Lpp-OmpA-eGFP-SC. Note that treatment with proteinase K led to degradation of the SC-ST complex (II) but not of mRFP-ST (I) expressed in the cytosol, thereby confirming that a substantial amount of the SC-ST complex is localized on the *E. coli* cell surface.

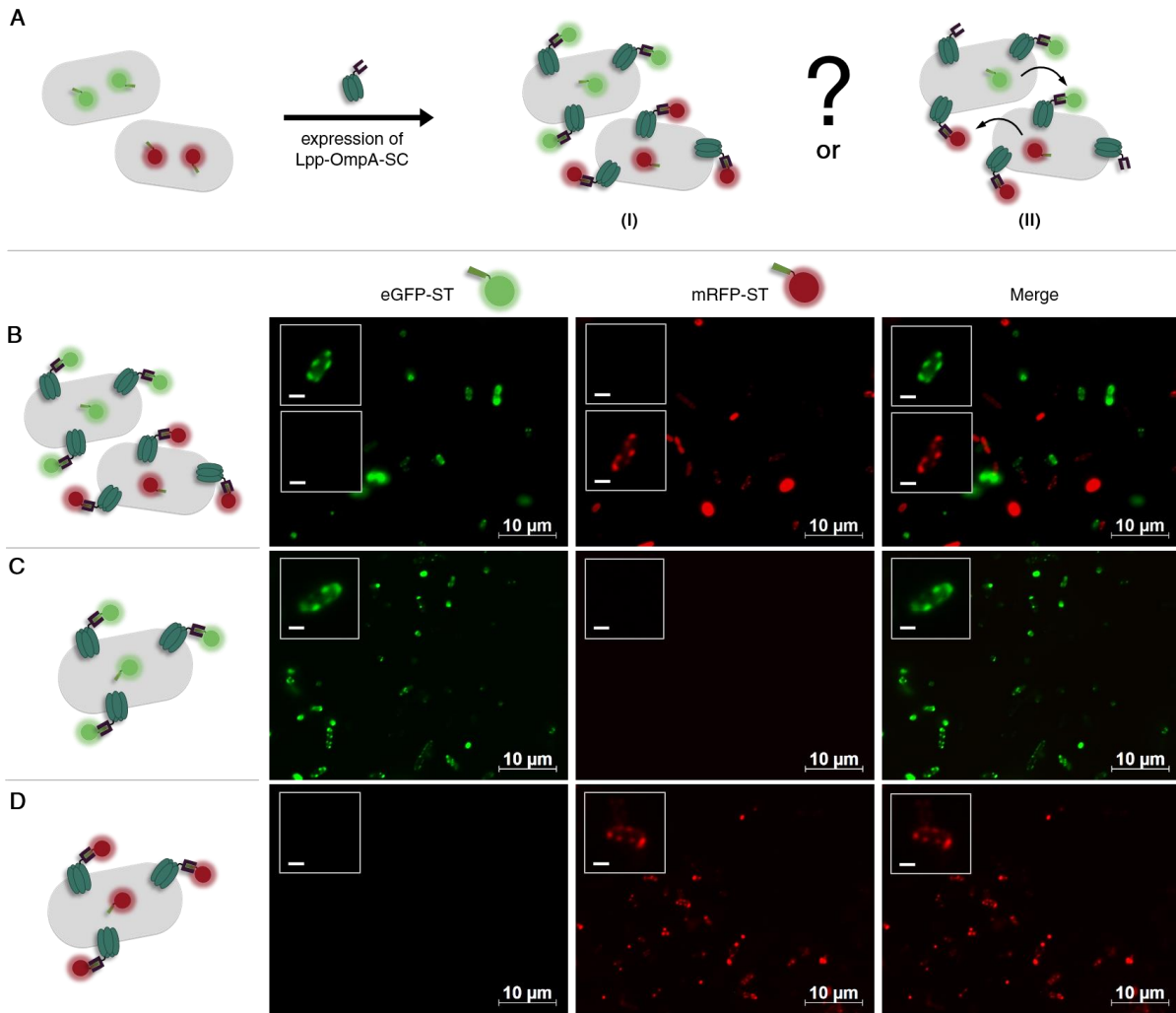


**Figure S3.** Fluorescence microscopic investigation of intercellular cross-coupling events. **(A)** Cells expressing eGFP-ST or mRFP-ST were co-cultured during expression of Lpp-OmpA-SC to investigate whether coupling of the fluorescent passenger-ST fusions with Lpp-OmpA-SC occurs exclusively intracellular *in situ* (I) or else by leakage of fluorescent passengers into the culture medium and subsequent coupling to surface presented Lpp-OmpA-SC fusions of surrounding cells (intercellular cross-coupling, II). The co-culture **(B)** only revealed cells of type (I), comparable to mono cultures of cells presenting eGFP-ST **(C)** or mRFP-ST **(D)**, indicating that no cross-coupling events occur. Scale bars in the magnified insets correspond to 1  $\mu$ m.

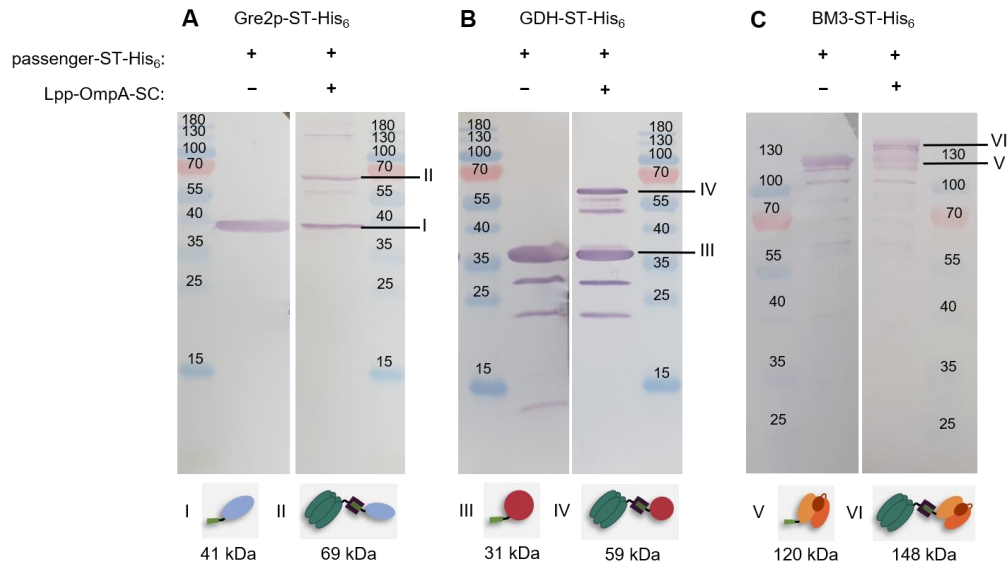


**Figure S4.** Conjugation of passenger enzymes Gre2p-ST (A), GDH-ST (B) and BM3-ST (C) to the membrane anchor Lpp-OmpA-SC. Whole-cell lysates of *E. coli* cells expressing passenger-ST fusions without (-) or with (+) induction of the Lpp-OmpA-SC expression were analyzed by western blot. Separation by SDS-PAGE and transfer to a PVDF membrane was followed by detection using primary mouse antibodies against His<sub>6</sub> and secondary anti-mouse antibodies conjugated to alkaline phosphatase. Although, a fraction of all passenger enzymes Gre2p-ST (I), GDH-ST (III) and BM3-ST (V) remained uncoupled, conjugation to the membrane anchor Lpp-OmpA-SC was confirmed for each passenger, as indicated by the higher molecular weight bands (II), (IV) and (VI) respectively, and is precisely controlled by the expression of Lpp-OmpA-SC. Note that for GDH-ST some lower molecular weight bands were detected presumably caused by degradation of the enzyme. Molecular weight of protein marker bands is given in kDa.

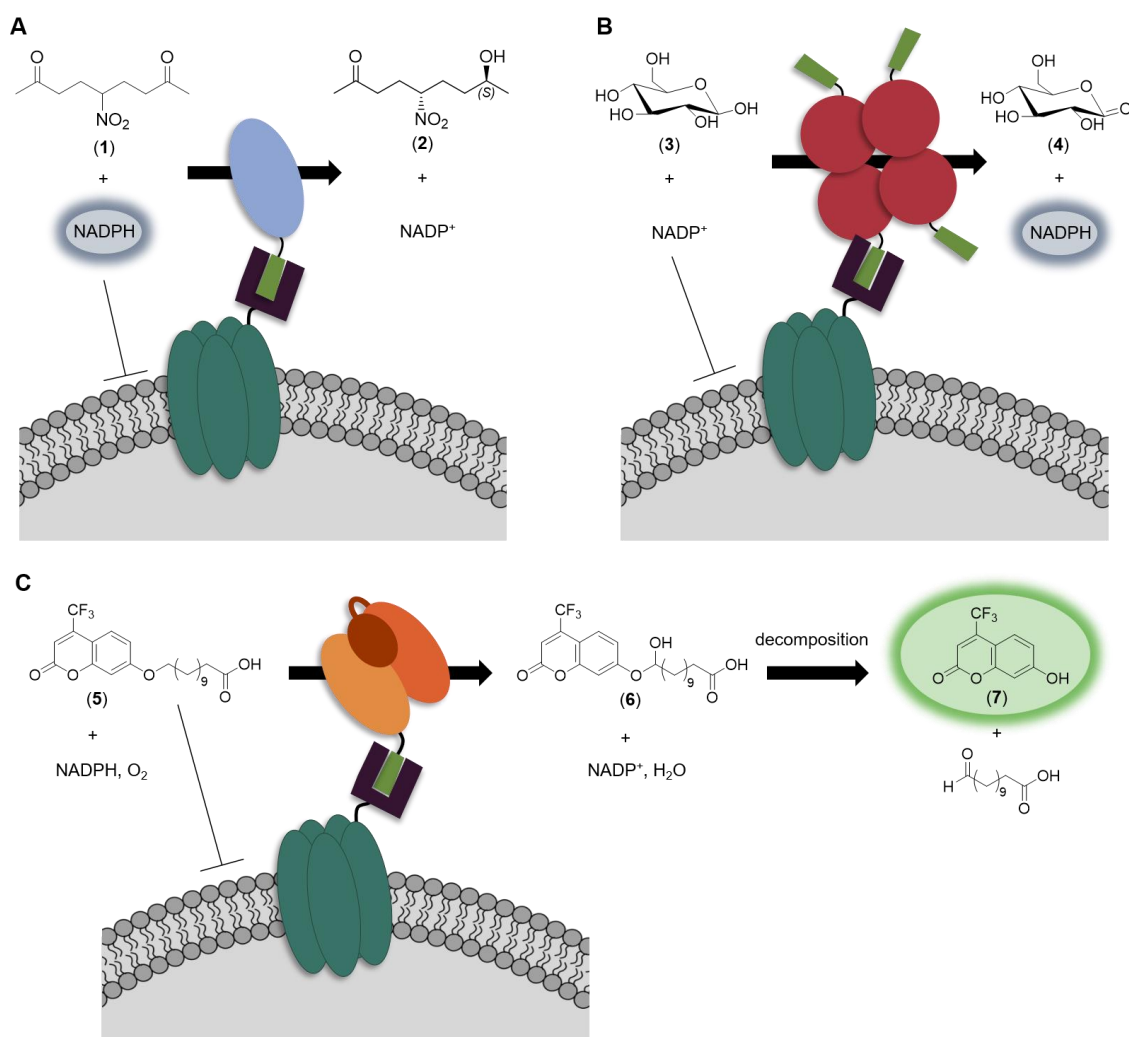


**Figure S5.** Conversion of membrane impermeable substrates or cofactors in fluorescence-based whole-cell biocatalytic activity assays. **(A)** Cells displaying Gre2p were incubated with 5-nitrononane-2,8-dione (**1**) and the fluorescent, membrane impermeable cofactor NADPH. The Gre2p-catalyzed conversion of (**1**) into (*S*)-anti hydroxyketone (**2**) was followed measuring the decrease in NADPH fluorescence. **(B)** GDH displaying cells were incubated with D-glucose (**3**) and the membrane impermeable cofactor NADP<sup>+</sup> and conversion of (**3**) into D-glucono-1,5-lactone (**4**) was followed measuring the increase in NADPH fluorescence. **(C)** Cells displaying BM3 were incubated with the membrane impermeable surrogate substrate 12-(4-trifluoromethylcoumarin-7-yloxy)dodecanoic acid (**5**) and the cofactor NADPH. BM3 catalyzed conversion of (**5**) leads to formation of the unstable hemiacetal intermediate (**6**) that spontaneously decomposes to release the fluorophore 7-hydroxy-4-trifluoromethylcoumarin (**7**). Note that in this study a BM3 variant carrying mutations A74G and F78V was used, which exhibits the highest reported conversion rate for the surrogate substrate (**5**).<sup>[8]</sup> The enzymatic conversions were followed by fluorescence read-out using a multi-mode microplate reader.

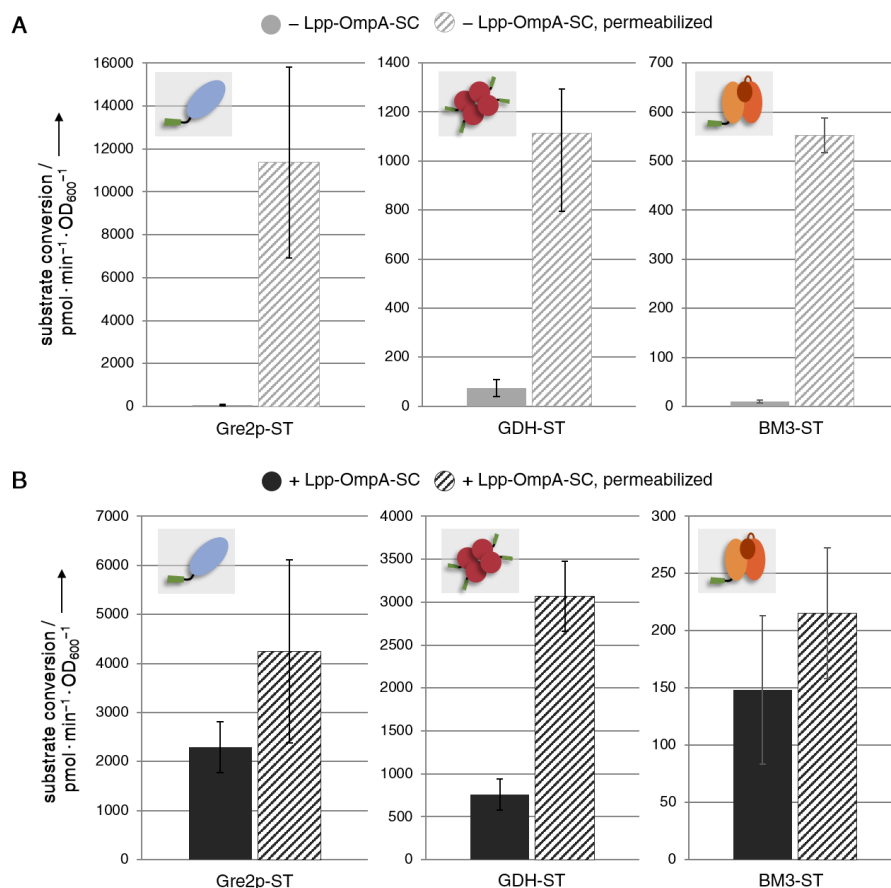


**Figure S6.** Whole-cell activities of intact and permeabilized *E. coli* cells expressing the passengers Gre2p-ST, GDH-ST and BM3-ST intracellularly (**A**) or else presenting the passengers on the cell surface after expression of Lpp-OmpA-SC (**B**). Substrate conversions were determined as illustrated in Figure S5. Cells were permeabilized by incubation with 2% toluene for 40 min. Error bars were obtained from at least two independent experiments. (**A**) Cells expressing the passengers intracellularly only convert the substrates after permeabilization with toluene, thus confirming that the chosen substrates are not able to penetrate into intact cells. (**B**) For cells displaying the passenger-ST fusions on their surface, the permeabilization led to a further increase in the conversion rate, presumably caused by excess uncoupled passenger enzymes that remained in the cytosol.

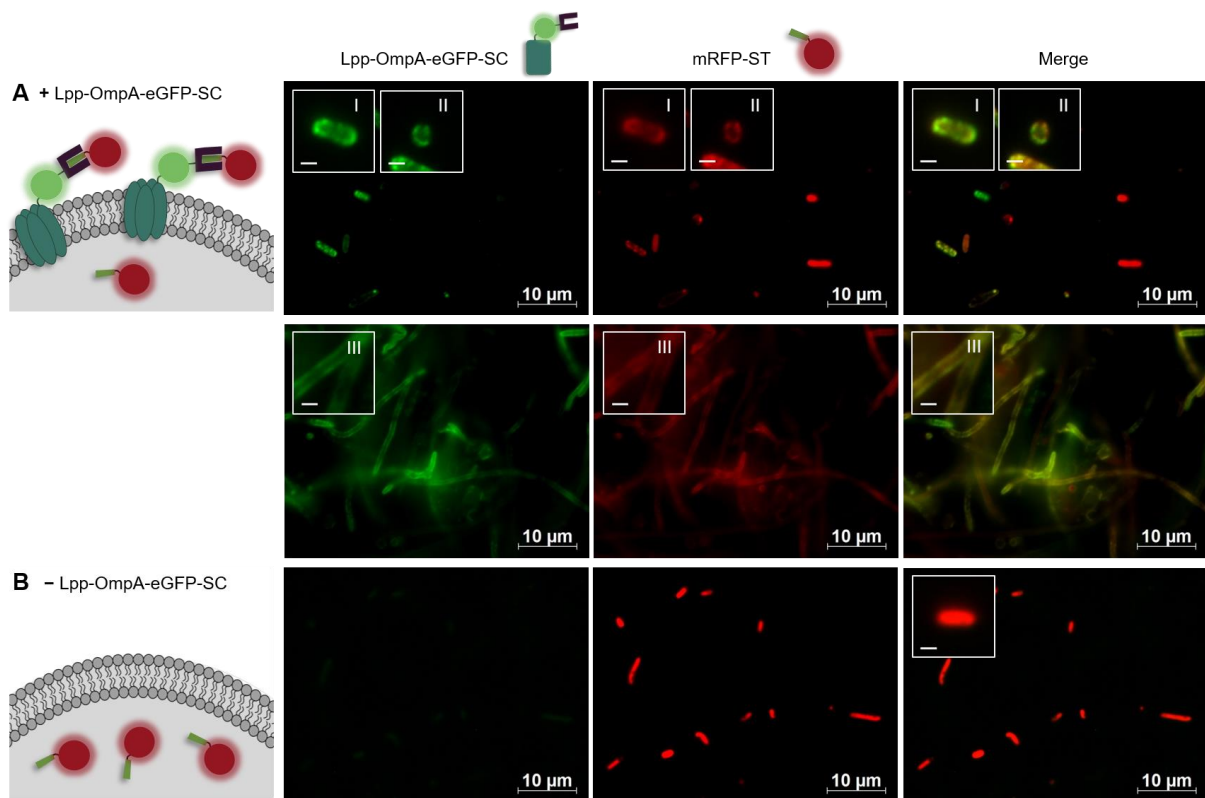


**Figure S7.** Fluorescence microscopy images of mRFP-ST and Lpp-OmpA-eGFP-SC expressing cells after 20 h of induction. **(A)** Various cell morphologies were observed in *E. coli* cells displaying mRFP-ST on their surface through interaction with Lpp-OmpA-eGFP-SC. Cells with normal (I) or spherical (II) shapes were detected as well as cells forming long filaments (III). **(B)** Controls, in which expression of Lpp-OmpA-eGFP-SC was not induced, showed regular shapes only. Scale bars in the magnified insets correspond to 1  $\mu\text{m}$ .

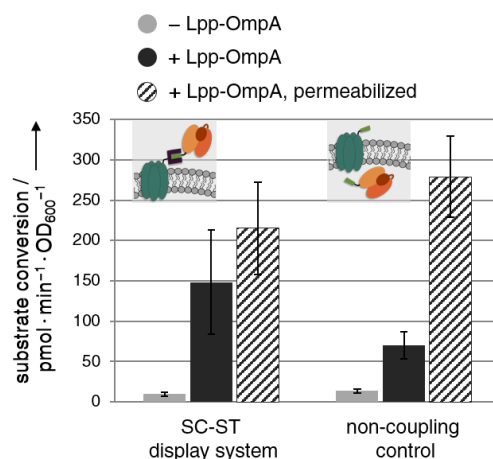


**Figure S8.** Whole-cell activities of *E. coli* cells displaying BM3 with the SC-ST display system and the corresponding non-coupling control. For gene constructs see Figure S1. Substrate conversions were determined as illustrated in Figure S5. Cells were analyzed without (– Lpp-OmpA) and with (+ Lpp-OmpA) expression of Lpp-OmpA-SC/Lpp-OmpA-ST fusions as well as after permeabilization by adding 2% toluene (+ Lpp-OmpA, permeabilized). Error bars were obtained from at least two independent experiments. Cells employing the non-coupling control, which overexpressed a Lpp-OmpA-ST fusion in the outer membrane and BM3-ST in the cytosol, showed conversion rates of the membrane impermeable substrate (5) that were about half as high as cells displaying BM3 on the cell surface with the SC-ST display system. This is presumably caused by modest cytosolic conversion of the substrate due to increased permeability of the *E. coli* outer membrane after overexpression of Lpp-OmpA fusions. After permeabilization of the cells with toluene a strong further increase in the conversion rate was observed for the non-coupling control, indicating that overexpression of Lpp-OmpA does not completely disrupt the membrane barrier.



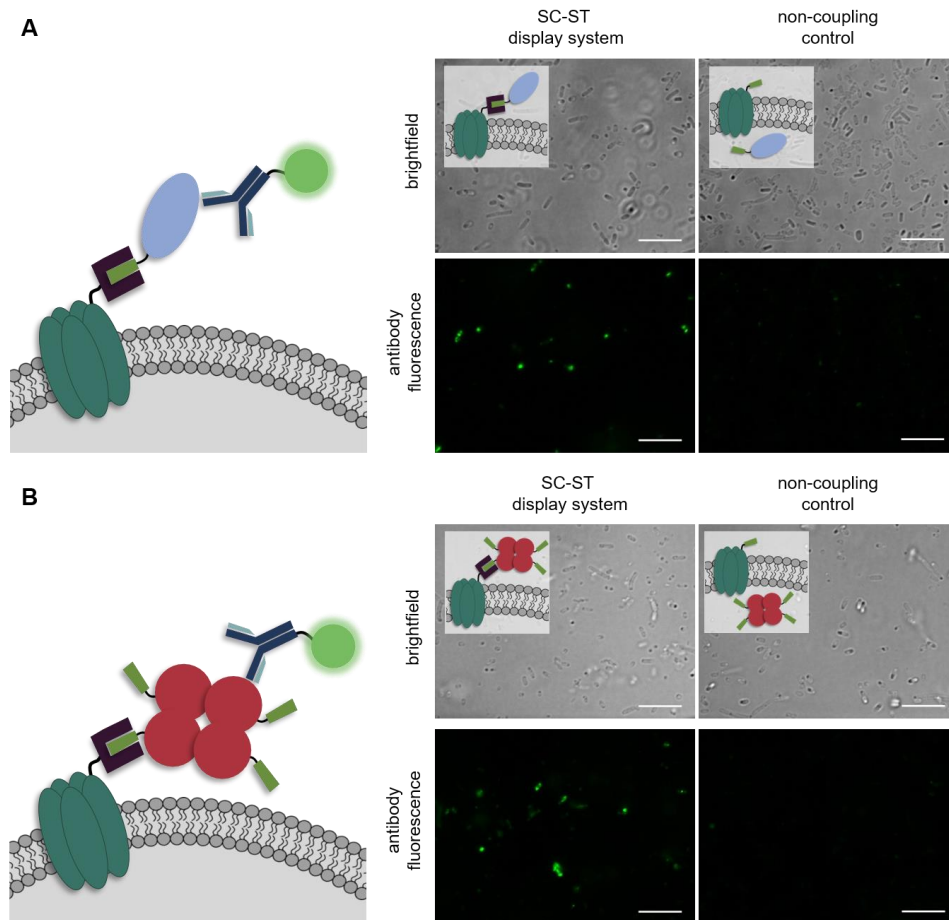


**Figure S9.** Verification of surface display of the passenger enzymes Gre2p (**A**) and GDH (**B**) by immunofluorescence microscopy. Gre2p-ST and GDH-ST fusions modified with C-terminal His<sub>6</sub> were detected using an anti-His<sub>6</sub> antibody conjugated to AlexaFluor488. Scale bars correspond to 10  $\mu$ m.

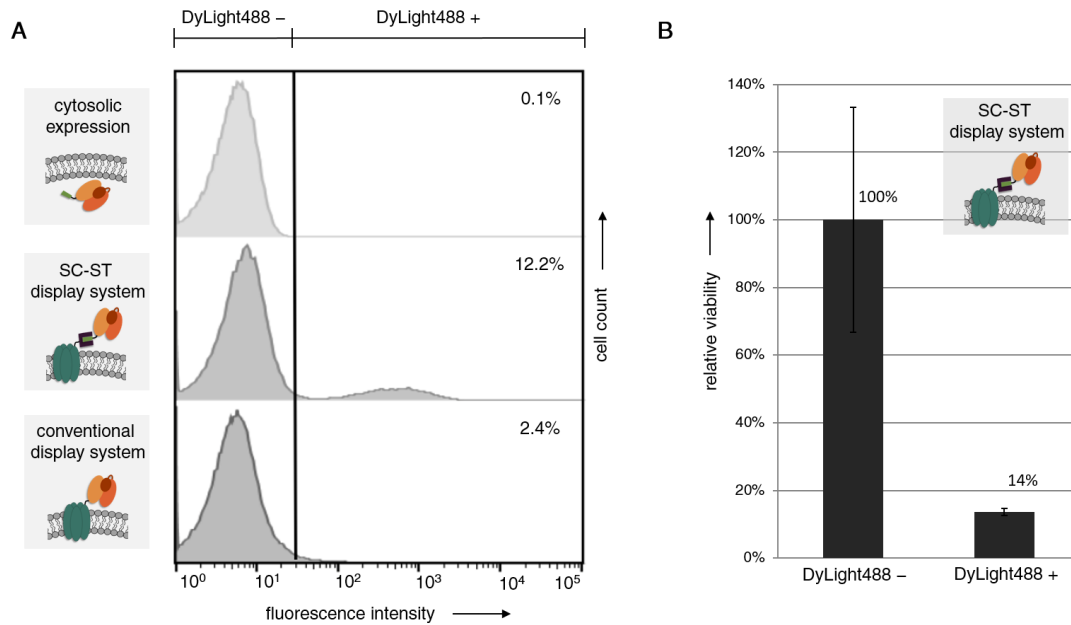


**Figure S10.** Flow cytometric analysis and sorting of cells displaying BM3. **(A)** Comparison of surface display efficiencies of the SC-ST and the conventional surface display system using flow cytometry. Reference cells expressing the passenger BM3-ST-Myc in the cytosol as well as cells displaying the passenger on their surface with the SC-ST or with the conventional display system were stained with an anti-myc antibody-DyLight488 conjugate. A significant proportion (12.2%) of cells displaying BM3 with the SC-ST display system were clearly stained with the antibody, while only 2.4% of cells displaying BM3 with the conventional display system exhibited very weak fluorescence. **(B)** In order to investigate the viability of cells displaying BM3 with the SC-ST display system, the same numbers of negative (DyLight488 -) and positive (DyLight488 +) cells were sorted onto different LB/agar plates and the viability was determined by counting the emerging colonies of two plates. Compared to cells that did not display the BM3 passenger on their surface (DyLight488 -), the viability was reduced to about 14% when the cells successfully displayed the BM3 passenger with the SC-ST display system (DyLight488 +). This reduced viability is in line with the observed alterations in membrane integrity caused by the L-arabinose induced overexpression of Lpp-OmpA (see Figure S8).

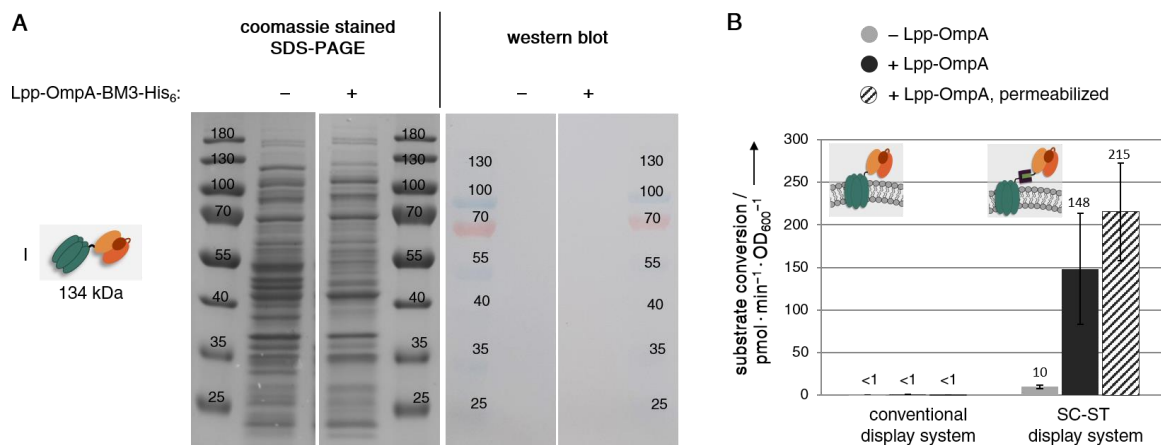


**Figure S11.** (A) Expression analysis of Lpp-OmpA-BM3-His<sub>6</sub> in the conventional display system. Whole-cell lysates were analyzed by coomassie stained SDS-PAGE (12% (w/v) acrylamide) and western blot analysis using primary mouse anti-His<sub>6</sub> antibodies and secondary anti-mouse antibodies conjugated to alkaline phosphatase. No expression was observed for the fusion protein Lpp-OmpA-BM3-His<sub>6</sub> (I) regardless of whether the expression was induced (+) or not (-). Molecular weight of protein marker bands is given in kDa. (B) Whole-cell activities of *E. coli* cells displaying BM3 with the conventional display system and the SC-ST display system. Substrate conversions were determined as illustrated in Figure S5. Cells were analyzed without (- Lpp-OmpA) and with (+ Lpp-OmpA) expression of Lpp-OmpA-BM3 or Lpp-OmpA-SC fusions as well as after permeabilization by adding 2% toluene (+ Lpp-OmpA, permeabilized). Error bars were obtained from at least two independent experiments. No substrate conversion was detected for the conventional display system even after permeabilization of the cells by toluene. Note that the data for the SC-ST display system is intended for comparison and is also shown in Figure S8.

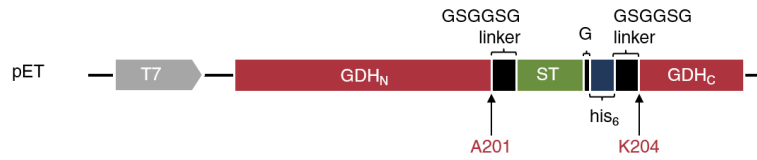


**Figure S12. Design of the GDH variant carrying an internal ST.** The GDH(ST) variant was constructed by inserting the ST and a his<sub>6</sub> sequence separated by a single glycine between the amino acids A201 and K204 of a flexible loop using GSGGSG sequences as linkers on both fusion sites. The native amino acids D202 and P203 were deleted.

## References

- [1] D. G. Gibson, L. Young, R.-Y. Chuang, J. C. Venter, C. A. r. Hutchison, H. O. Smith, *Nat. Methods* **2009**, *6*, 343–345.
- [2] R. E. Campbell, O. Tour, A. E. Palmer, P. A. Steinbach, G. S. Baird, D. A. Zacharias, R. Y. Tsien, *Proc. Natl. Acad. Sci. U. S. A.* **2002**, *99*, 7877.
- [3] T. Peschke, K. S. Rabe, C. M. Niemeyer, *Angew. Chem., Int. Ed. Engl.* **2017**, *56*, 2183–2186.
- [4] T. Peschke, M. Skoupi, T. Burgahn, S. Gallus, I. Ahmed, K. S. Rabe, C. M. Niemeyer, *ACS Catal.* **2017**, *7*, 7866–7872.
- [5] T. Peschke, P. Bitterwolf, S. Gallus, Y. Hu, C. Oelschlaeger, N. Willenbacher, K. S. Rabe, C. M. Niemeyer, *Angew. Chem., Int. Ed. Engl.* **2018**, *57*, 17028–17032.
- [6] M. Erkelenz, C.-H. Kuo, C. M. Niemeyer, *J. Am. Chem. Soc.* **2011**, *133*, 16111–16118.
- [7] M. Skoupi, C. Vaxelaire, C. Strohmann, M. Christmann, C. M. Niemeyer, *Chemistry* **2015**, *21*, 8701–8705.
- [8] K. Neufeld, S. M. z. Berstenhorst, J. Pietruszka, *Analyt. Biochem.* **2014**, *456*, 70–81.